Soft Condensed Matter

New Research

Contributors

R. An
B. Brutovsky
S. V. Chong
Patrícia F. N. Faísca
Nélido González-Segredo
B. Ingham
Z. C. Ou-Yang
George D. J. Phillies
A. E. Sitnitsky
Hidetaka Sonoda
Kiril A. Streletzky
J. L. Tallon
V. Lisy
J. Tothova
Z. C. Tu
Enis Tuncer
Gentaro Watanabe
Michael Wegener
Vladimir A. Yurovsky
A. V. Zatovsky

Kathy I. Dillon
Editor

NOVA

Library of Congress Cataloging-in-Publication Data

Soft condensed matter : new research / Kathy I. Dillon (editor).
p. cm.
Includes index.
ISBN 13: 978-1-59454-665-5
ISBN 10: 1-59454-665-7
1. Soft condensed matter--Research. I. Dillon, Kathy I.
QC173.458.S62S64 2006
530.4'1072--dc22 2005029403

Published by Nova Science Publishers, Inc. ✣New York

SOFT CONDENSED MATTER: NEW RESEARCH

PREFACE

Condensed matter is one of the most active fields of physics, with a stream of discoveries in areas from superfluidity and magnetism to the optical, electronic and mechanical properties of materials such as semiconductors, polymers and carbon nanotubes. It includes the study of well-characterized solid surfaces, interfaces and nanostructures as well as studies of molecular liquids (molten salts, ionic solutions, liquid metals and semiconductors) and soft matter systems (colloidal suspensions, polymers, surfactants, foams, liquid crystals, membranes, biomolecules etc) including glasses and biological aspects of soft matter. This new book presents state-of –art research in this exciting field.

More than twenty years ago, it was predicted that nuclei can adopt interesting shapes, such as rods or slabs, etc., in the cores of supernovae and the crusts of neutron stars. These non-spherical nuclei are referred to as nuclear "pasta." In recent years, we have been studying the dynamics of the pasta phases using a method called quantum molecular dynamics (QMD) and have opened up a new aspect of study for this system. Our findings include: dynamical formation of the pasta phases by cooling down the hot uniform nuclear matter; phase diagrams in the density versus temperature plane; structural transitions between the pasta phases induced by compression and elucidation of the mechanism by which they proceed. In the Chapter 1, we give an overview of the basic physics and astrophysics of the pasta phases and review our works for readers in other fields.

The dynamics of individual polymers in solution is fundamental for understanding the properties of polymeric systems. Consequently, considerable work has been devoted towards understanding polymer dynamics. In spite of the long-standing investigations, a number of problems remains between the theory and experiments, such as the dynamic light or neutron scattering. For example, the value of the first cumulant of the dynamic structure factor (DSF) is lower than the theoretical prediction for flexible polymers. The origin of these discrepancies is a matter of continuous discussion. The development of the theory of polymer dynamics is thus still of interest.

Chapter 2 represents an attempt of such a development. The main idea of the proposed generalization comes from the theory of the Brownian motion, which lies in the basis of the bead-spring models of polymer dynamics. In the classical (Einstein) description the resistance force on the bead moving in a liquid is the Stokes force, which is valid only for the steady motion. In a more general nonstationary case the hydrodynamic memory, which is a consequence of fluid inertia, should be taken into account. In the Brownian motion it displays in the famous "long-time tails" in the velocity autocorrelation function. The time dependence of the mean square displacement (MSD) of the particle changes from the "ballistic" regime at

short times to the Einstein diffusion at long times. We have found similar effects in the dynamics of polymers. We give the corresponding generalization of the Rouse-Zimm (RZ) theory. It is shown that the time correlation functions describing the polymer motion essentially differ from those in the RZ models. The MSD of the polymer coil is at short times proportional to t^2 (instead of t). At long times it contains additional (to the Einstein term) contributions, the leading of which is $\sim t^{1/2}$. The relaxation of the internal normal modes of the polymer differs from the traditional exponential decay. This is displayed in the tails of their correlation functions, the longest-lived being $\sim t^{-3/2}$ in the Rouse limit and $t^{-5/2}$ in the Zimm case when the hydrodynamic interaction is taken into account. It is discussed that the found peculiarities, in particular a slower diffusion of the coil, should be observable in dynamic scattering experiments. The DSF and the first cumulant of the polymer coil are calculated. Finally, we extend the theory to the situation when the dynamics of the studied polymer is influenced by the presence of other polymers in dilute solution.

Bose-Einstein condensate (BEC) is considered under conditions of Feshbach resonance in two-atom collisions due to a coupling of atomic pair and resonant molecular states. The association of condensate atoms can form a molecular BEC, and the molecules can dissociate to pairs of entangled atoms in two-mode squeezed states. Both entanglement and squeezing can be applied to quantum measurements and information processing.

In Chapter 3, the processes in the atom-molecule quantum gas are analyzed using two theoretical approaches. The mean-field one takes into account deactivating collisions of resonant molecules with other atoms and molecules, neglecting quantum fluctuations. This method allows analysis of inhomogeneous systems, such as expanding BEC. The non-mean-field approach — the parametric approximation — takes into account both deactivation and quantum fluctuations. This method allows determination of optimal conditions for formation of molecular BEC and describes Bose-enhanced dissociation of molecular BEC, as well as entanglement and squeezing of the non-condensate atoms.

In Chapter 4, after introducing amphiphilic fluids and their technological and fundamental relevance, I focus attention on reviewing recent amphiphilic fluid research carried out using five different mesoscopic methods, namely, coarse-grained molecular dynamics, lattice-gas automata, lattice-Boltzmann, dissipative particle dynamics and stochastic rotation dynamics. Their *leit motif* is to pick out the atomistic detail most relevant for self-assembly and the emergence of hydrodynamics, and to map out the model's parameter space. I give an account of each one's strengths and weaknesses, and suggest ways forward by pointing out phenomenology hitherto untackled by the computational modeller.

In Chapter 5, the role of the rigidity of a peptide chain in its equilibrium dynamics is investigated within a realistic model with stringent microscopically derived coupling interaction potential and effective on-site potential. The coupling interaction characterizing the chain rigidity and the effective on-site potentials are calculated for three main types of protein secondary structure. The coupling interaction is found to be surprisingly weak for all of them but different in character: repulsive for β-helix and anti-parallel β-sheet structures and attractive for parallel β-sheet structure. The effective on-site potential is found to be a hard one for β-helix and anti-parallel β-sheet and a soft one for parallel β-sheet. In all three types of protein secondary structures a stable zig-zag shape discrete breather (DB) associated with the oscillations of torsional (dihedral) angles can exist due to weakness of the coupling interaction. However, since the absorption of far infrared radiation (IR) by proteins is known

to require the existence of rather long chains of hydrogen bonds that takes place only in β-helicies, then one can conclude that the excitation of a DB in such a way is possible in β-helix and seems to be hardly possible in β-sheet structures. The interpretation of the recent experiments of Xie et al. on far IR laser pulse spectroscopy of proteins is suggested. The frequency of a DB in an the β-helix is obtained in the region of 115 cm^{-1} in accordance with these experiments.

Organic-inorganic hybrid materials based on simple two-dimensional layers of tungsten oxide separated by organic molecules are merely one example of the huge variety of systems classed as "organic-inorganic hybrids". The materials in question have the potential to combine the high-electron mobility of the metal oxide layers with the flexibility of the organic layers. More importantly they identify the primary elements that might enable the formation of more complex nanostructures through self-assembling processes and the templating effect of the organic component. One such example that will be discussed here is the possibility of including magnetic ions within the inorganic layers, which is observed to have profound effects upon the magnetic behaviour of the resulting hybrids.

Tungsten oxide-organic amine hybrid materials have been synthesised via a range of methods and characterised using conventional materials characterisation techniques, such as X-ray diffraction, infrared and Raman spectroscopy, UV-visible spectroscopy and electron microscopy. Chapter 6 is also complemented by *ab initio* calculations of the physical and electronic structure of the tungsten oxide hybrids. For compounds incorporating transition metal elements, the magnetisation was also measured. The effect of the low-dimensionality of the inorganic component is clearly seen in materials that include certain transition metals, in the form of magnetic transitions that indicate a crossover from 2-dimensional to 3-dimensional behaviour.

As explained in Chapter 7, understanding the process according to which a linear polypeptide chain acquires its highly structured, biologically functional native fold is one of the most fundamental problems in science. Considerable insight into the physics of the folding process was gained from the study of simplified protein models and the use of computer simulations. The energy landscape theory of protein folding, which is largely the result of this approach, provided a theoretical framework which led to the emergence of new concepts (e.g., the transition state ensemble, the folding funnel, etc) and stimulated an invaluable synergy between theoretical and experimental research in the folding problem. An important development resulting from such an integrated approach is the key idea that the native topology has a dominant role in determining the kinetics and mechanisms of small, single domain, two-state folders. Such a surprising simplicity suggests in turn that the underlying physics of the folding process can indeed be described by relatively simple protein models.

Experimental measurements of static and dynamic properties of non-ionic polymer solutions provide good testing grounds for existing and new models of polymer solution dynamics. We extensively studied aqueous solutions of the high molecular weight, rodlike, semiflexible polymer hydroxypropylcellulose (HPC). In Chapter 8 we present our systematic analysis of measurements of: a) low-shear viscosity η, b) quasi-elastic light scattering spectra of HPC solutions, including mode structure analysis at a range of temperatures and concentrations, c) quasi-elastic light scattering spectra of optical probe particles diffusing

through HPC solutions, including careful characterization of modes of diffusive relaxation for tracer particles of different sizes, and d) static light scattering.

We found a variety of novel phenomena. (i) The functional dependence of η on concentration has a transition at c^+, with disparate small- and large- concentration dependences being seen. For $c < c^+$, η depends on c via a stretched exponential $\exp(-ac_V)$ in c ("solution-like" behavior). For $c > c^+$, η depends on c via a power law $\eta \sim c^x$ with $x \approx 4$ ("meltlike" behavior). The viscometric crossover at c_+ is echoed by the probe diffusion data, confirming the physical reality of the solutionto- meltlike transition. (ii) Optical probe spectra and polymer spectra are both strongly non-exponential and can be decomposed into two or (at larger polymer concentrations) three spectral modes. Mode structure analysis reveals that probe relaxations and polymer relaxations in the same solution sample different aspects of polymer dynamics. (iii) Except for the largest (0.76μm) probes, diffusion coefficients of tracer particles in polymer solutions are not determined by the solution macroscopic viscosity. (iv) At concentrations above c^+, light scattering spectra of HPC in solution have an ultraslow relaxational mode. This mode exhibits properties expected for long-lived dynamic structures but not the properties expected for local equilibrium regions of elevated polymer concentration. Properties of the slow mode are consistent with predictions from some models of glass formation. Finally, (v) polymer solutions have a characteristic dynamic length, which is approximately the hydrodynamic radius of the polymer.

Polymeric materials play an important role in daily life due to possibilities of tailoring special materials based on their unique properties, *e.g.*, processability, light weight, electrically/thermally insulating, chemical resistivity, mechanical softness, shock absorbing *etc.* In addition to massive, large-scale, bulk applications as packaging materials, cables, pipes *etc.*, technological applications based on special polymers have been emerged, for example in the case of employing active thin polymeric layers to convert mechanical energy to electricity or the opposite to convert electrical energy to mechanical stress. These electro-mechanical (also known as piezoelectric) polymers are introduced in a broad variety of electro-acoustic and electro-mechanical applications. Some examples are ultrasonic transducers in medician, defect characterization sensors, microphones, car air-bag sensors, shock-wave transducers, surveillance and traffic sensors, touch pads and panels, *etc.* The prevalent polymeric materials for electromechanical tranducer applications are polyvinylidene fluoride and its copolymers, and cellular polypropylene. The origin of the electro-mechanical activity in these polymers are quite different. The piezoelectricity in the former materials are caused by the change in their electrical dipole density, created by the oriented polar molecules, when a mechanical stress is applied; these materials belong to ferroelectrics. Unlike polyvinylidene fluoride based materials, which have been well-investigated in the last forty years, cellular polypropylene has recently shown a ferroelectric-like behavior. The polarizable units in cellular polypropylene are macroscopic charged voids, which generate the so-called *'ferroelectret'* behavior. One of the advantages of cellular polypropylene over others is that the internal structure of cellular films can be modified to increase the electro-mechanical activity, up-to ten times higher than polyvinylidene fluoride based materials. To better understand the physics behind and to be able to design special cellular materials for transducer applications computer simulations are vital. In the computer model, one should not only include the properties of constituents, *e.g.* polypropylene and the void, but also the arrangement of the constituents in the materials (the actual topology). Once these parameters

are known, it is trivial to simulate (predict) the behavior of the material system under different physical conditions, it would otherwise be expensive and time consuming in trial-and-error experimental techniques. In Chapter 9, we will first present briefly the preparation process of the cellular films, later will give the essential steps to model, to predict and to design softmaterials for electro-mechanical applications. We will first concentrate on, separately, electrical and mechanical aspects of material modeling. Later, the coupling of these stress fields and their importance in understanding the properties of materials used in the electro-mechanical applications will be presented.

A cell membrane can be simplified as a composite film consisting of lipid bilayer, membrane skeleton beneath the lipid bilayer, and proteins embedded in the lipid bilayer and linked with the membrane skeleton if one only concerns its mechanical properties. In Chapter 10, above all, the authors give a brief introduction to some important results on mechanical properties of lipid bilayers following Helfrich's seminal work on spontaneous curvature energy of lipid bilayers. Next, the entropy of a chainlike polymer confined in a curved surface and the free energy of membrane skeleton are obtained by scaling analysis. It is found that the free energy of cell membranes has the form of the in-plane strain energy plus Helfrich's curvature energy. The equations to describe equilibrium shapes and in-plane strains of cell membranes by osmotic pressures are obtained by taking the first order variation of the total free energy containing the elastic free energy, the surface tension energy and the term induced by osmotic pressure. The stability of spherical cell membranes is discussed and the critical pressure is found to be much larger than that of spherical lipid bilayers without membrane skeleton. Lastly, the authors try to extend the present static mechanical model of cell membranes to the cell structure dynamics by proposing a group of coupling equations involving the tensegrity architecture of cytoskeleton, the fluid dynamics of cytoplasm and elasticities of cell membranes.

CONTENTS

Preface		**vii**
Chapter 1	Dynamical Simulation of Nuclear "Pasta": Soft Condensed Matter in Dense Stars *Gentaro Watanabe and Hidetaka Sonoda*	**1**
Chapter 2	The Dynamics of Polymers in Solution with Hydrodynamic Memory *V. Lisy, J. Tothova, B. Brutovsky and A.V. Zatovsky*	**35**
Chapter 3	Formation of Molecules and Entangled Atomic Pairs from Atomic BEC due to Feshbach Resonance *Vladimir A. Yurovsky*	**79**
Chapter 4	Amphiphilic Fluids: Mesoscopic Modelling and Computer Simulations *Nélido González-Segredo*	**125**
Chapter 5	Discrete Breathers in Protein Secondary Structure *A.E. Sitnitsky*	**157**
Chapter 6	Organic-Inorganic Layered Hybrid Materials *B. Ingham, S.V. Chong and J.L. Tallon*	**173**
Chapter 7	Shaping Protein Folding Dynamics with Native State's Geometry *Patrícia F. N. Faísca*	**195**
Chapter 8	Dynamics of Semirigid Rod Polymers from Experimental Studies *George D.J. Phillies and Kiril A. Streletzky*	**219**
Chapter 9	Soft Polymeric Composites for Electro-mechanical Applications: Predicting and Designing Their Properties by Numerical Simulations *Enis Tuncer and Michael Wegener*	**265**

Chapter 10 Elasticities and Stabilities: Lipid Membranes vs Cell Membranes **325**
Z.C. Tu, R. An and Z.C. Ou-Yang

Index **339**

In: Soft Condensed Matter: New Research
Editor: Kathy I. Dillon, pp. 1-33
ISBN 1-59454-665-7

Chapter 1

DYNAMICAL SIMULATION OF NUCLEAR "PASTA": SOFT CONDENSED MATTER IN DENSE STARS

Gentaro Watanabe[a,b] ***and Hidetaka Sonoda***[c,b]
[a]NORDITA, Blegdamsvej 17, DK-2100 Copenhagen Ø, Denmark
[b]The Institute of Chemical and Physical Research (RIKEN)
Saitama 351-0198, Japan
[c]Department of Physics, University of Tokyo, Tokyo 113-0033, Japan

Abstract

More than twenty years ago, it was predicted that nuclei can adopt interesting shapes, such as rods or slabs, etc., in the cores of supernovae and the crusts of neutron stars. These non-spherical nuclei are referred to as nuclear "pasta."

In recent years, we have been studying the dynamics of the pasta phases using a method called quantum molecular dynamics (QMD) and have opened up a new aspect of study for this system. Our findings include: dynamical formation of the pasta phases by cooling down the hot uniform nuclear matter; phase diagrams in the density versus temperature plane; structural transitions between the pasta phases induced by compression and elucidation of the mechanism by which they proceed. In the present article, we give an overview of the basic physics and astrophysics of the pasta phases and review our works for readers in other fields.

1. Introduction

Massive stars with masses $M = 8 - (30 - 50)M_\odot$ ($M_\odot$ is the mass of the sun) end their lives in the most spectacular and violent events in the Universe: explosions called supernovae, which are driven by gravitational collapse of the stellar core (see, e.g., Ref. [56]). The mechanism for the collapse-driven supernova explosion has been a central mystery in astrophysics for almost half a century [12].

Great efforts have been made to unravel the mystery and a qualitative picture has been obtained so far (see, e.g., Refs. [6, 59, 70, 71, 72]). We now know that after supernova explosions the collapsing core becomes a dense compact object, neutron star, for $M = 8 - 30M_\odot$ or further collapses to a black hole for $M \gtrsim 30M_\odot$. However, no calculations incorporating reasonable physical input succeeded in reproducing an explosion; in

the calculations, shock waves stall on their way out of the collapsing core and the core does not explode but contracts into a black hole. These earlier studies suggest that interactions between neutrinos from the central region of the star and the shocked matter are important for the success of an explosion. This will hopefully revive the shock wave, and lead to a successful explosion.

In equilibrium dense matter in supernova cores and neutron stars, the existence of nuclei with rod-like and slab-like shape is predicted [20, 52]. Such nuclei with exotic shapes are referred to as nuclear "pasta." The nuclear pasta itself is an interesting subject from the point of view of materials science of dense stellar matter and it has been studied by nuclear physicists in addition to astrophysicists for more than twenty years. Furthermore, the pasta phases have recently begun to attract the attention of many researchers (see, e.g., Refs. [9, 35] and references therein). As has been pointed out in Refs. [55, 64, 66] and elaborated in Refs. [22, 23, 57], the existence of the pasta phases modifies the interaction between neutrinos and matter significantly. Our recent work [65] strongly suggests the possibility of dynamical formation of the pasta phases in collapsing cores from a crystalline lattice of spherical nuclei; effects of the pasta phases on the supernova explosions should be seriously discussed in the near future.

In the present article, we provide an overview of the physics and astrophysical background of the pasta phases for researchers in other fields, especially in soft condensed matter physics. We try to show that the pasta phases can be an interesting system for many researchers in various fields, not only for nuclear astrophysicists. The plan of this paper is as follows. In the remaining part of the present section, we first give a brief explanation of collapse-driven supernovae, neutron stars and materials in these objects. We then describe the basic physics and astrophysical consequences of the pasta phases. In Section 2., we discuss the similarity between the pasta phases and soft condensed matter. We then explain a theoretical framework used in our studies in Section 3., and show the results in Section 4.. In this article, we generally set the Boltzmann constant $k_{\rm B} = 1$.

1.1. Collapse-Driven Supernovae

Stars evolve by burning light elements into heavier ones (see, e.g., Ref. [71]); here burning means nuclear fusion. The ultimate fate of the star is basically determined by its mass in the main sequence period, when the star is supported by thermal pressure of burning hydrogen nuclei (protons). Nuclear reactions of heavier nuclei require higher temperatures because of their greater Coulomb barrier. In the core of massive stars with $M \gtrsim 8M_{\odot}$, the temperature reaches a threshold to produce iron. Elements heavier than iron cannot be produced by nuclear fusion since the binding energy per nucleon of iron is the greatest among all the elements. Therefore iron nuclei, the major final product of a chain of the thermally driven nuclear reactions, accumulate in the core of massive stars at the end of their evolution.

As the nuclear burning proceeds and the mass of the iron core increases, two processes which tend to make the core unstable to collapse occur — electron capture, and photodissociation of heavy nuclei. In the iron core the density is so high ($\sim 4 \times 10^9 \mathrm{g\,cm^{-3}}$) that the core is supported mainly by electron degeneracy pressure; degenerate electrons have extremely large momenta even at zero temperature due to the Pauli exclusion principle. When

the electron Fermi energy exceeds 3.7 MeV, electron capture on iron nuclei occurs:

$$^{56}\mathrm{Fe} + \mathrm{e}^{-} \rightarrow {}^{56}\mathrm{Mn} + \nu_{\mathrm{e}} \, . \tag{1}$$

Since this reaction decreases the electron density, the electron degeneracy pressure decreases and can no longer support the iron core. This instability leads to contraction of the core. The other instability is triggered by photodissociation of iron nuclei, which occurs when the temperature of the core is $\gtrsim 5 \times 10^9$ K:

$$\gamma + {}^{56}_{26}\mathrm{Fe} \rightarrow 13\alpha + 4\mathrm{n} - 124.4\mathrm{MeV} \, . \tag{2}$$

This is an endothermic reaction; thus it decreases the gas pressure and accelerates the collapse.

As the collapse of the core proceeds and the central density approaches the nuclear saturation density (normal nuclear density), $\rho_0 = 0.165$ nucleons fm$^{-3} \simeq 3 \times 10^{14}$ g cm^{-3}, the equation of state suddenly becomes hard because of a strong short-range repulsion between nucleons. Due to this hardening, the pressure becomes sufficiently high to halt the collapse, causing the inner region of the core to bounce. The outer region of the core continues to fall towards the center at supersonic velocities. Consequently, the bouncing inner core drives a shock wave into the infalling outer core. The initial energy of the shock is $\sim 10^{51}$ erg and is enough to blow off the stellar envelope, which results in an explosion of the star. However, the shock wave propagating through the outer core is weakened by several processes (see, e.g., Ref. [59]) which decrease the pressure and dissipate the energy behind the shock front. Consequently, the shock wave stalls in the outer core. Neutrinos emitted from the inner core will heat the matter behind the shock front (a process referred to as neutrino heating). If the neutrino heating is efficient enough, the stalled shock can be revived, reach the surface of the outer core, propagate beyond the core, and finally blow off the outer layer of the star; thereby producing a supernova explosion. The contracted core remains as a nascent neutron star.

The difference in the gravitational energy between the iron core and a neutron star is given by

$$\Delta E \simeq -\left(\frac{GM_{\mathrm{core}}^2}{R_{\mathrm{Fe\ core}}} - \frac{GM_{\mathrm{core}}^2}{R_{\mathrm{NS}}} \right) \simeq \frac{GM_{\mathrm{core}}^2}{R_{\mathrm{NS}}} \sim O(10^{53}) \ \mathrm{erg} \, , \tag{3}$$

where G is the gravitational constant, $M_{\mathrm{core}} \sim 1 M_{\odot}$ is the mass of the core, $R_{\mathrm{Fe\ core}} \sim O(10^3)$ km is the initial radius of the iron core and the neutron star radius R_{NS} is about 10 km. Only one percent of this energy is injected into the gas blown off and 99 % is carried away by neutrinos [1]. In the supernova explosion, neutrinos interact with matter and will inject kinetic energy into it. Therefore detailed investigations of interactions between neutrinos and matter in supernova cores are necessary to understand the explosion mechanism (see, e.g., Refs. [6, 9, 18, 35]).

As the density in the core increases during the collapse, the mean free path of neutrinos l_ν decreases mainly due to the neutrino coherent scattering from nuclei via the weak neutral current. The amplitude of the coherent scattering is proportional to A, where A is the mass

[1] The gravitational energy is emitted in all six flavors of neutrinos and anti-neutrinos almost equally. However, muon and tauon neutrinos (and anti-neutrinos) are not important for supernova explosions because they interact with matter extremely weakly. Thus, hereafter, the term "neutrino" denotes an electron neutrino.

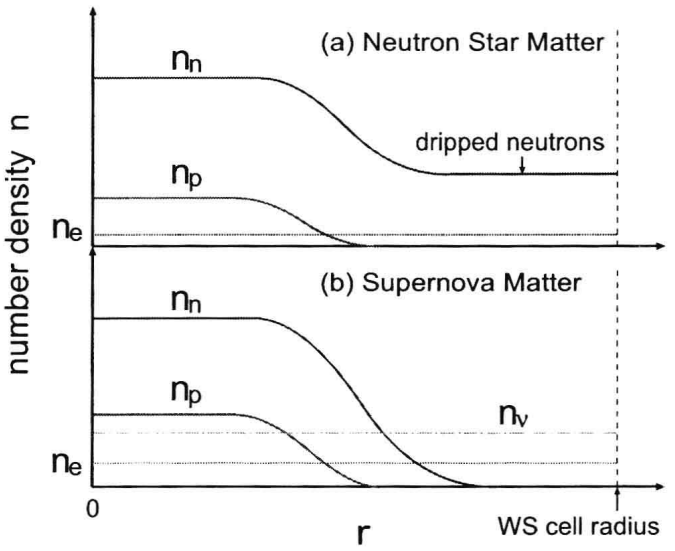

Figure 1. (Color) Schematic diagram of a Wigner-Seitz cell of neutron star matter (NSM) and supernova matter (SNM) where $n_{\rm n}$, $n_{\rm p}$, $n_{\rm e}$ and n_ν are the number densities of neutrons, protons, electrons and neutrinos respectively.

number of the nucleus. Therefore its cross section σ is proportional to A^2 [17], while that of the incoherent scattering is simply proportional to A. When the neutrino wavelength is much longer than the radius of the nucleus, the neutrino is coherently scattered by nucleons in the nucleus. In the collapsing iron core, a typical value of the wavelength λ_ν of a neutrino with energy E_ν is

$$\lambda_\nu = \frac{hc}{E_\nu} \simeq 2\pi \times 20\,\mathrm{fm} \left(\frac{10\mathrm{MeV}}{E_\nu}\right), \tag{4}$$

and that of the nuclear radius $r_{\rm N}$ is

$$r_{\rm N} \simeq 1.2A^{1/3}\,\mathrm{fm} \simeq 5\,\mathrm{fm} \left(\frac{A}{56}\right)^{1/3}. \tag{5}$$

The neutrino diffusion time scale is estimated by the random-walk relation:

$$\tau_{\rm diff} \sim \frac{R^2}{cl_\nu}, \tag{6}$$

where R is the radius of the collapsing core and c is the speed of light. The dynamical time scale of the core collapse is comparable to the free-fall time scale:

$$\tau_{\rm dyn} \sim \frac{1}{\sqrt{G\rho_{\rm core}}}, \tag{7}$$

where $\rho_{\rm core}$ is the density of the core. When $\tau_{\rm diff}$ is greater than $\tau_{\rm dyn}$ (the corresponding density region is above $10^{11-12}\mathrm{g\,cm^{-3}}$), neutrinos cannot escape from the inner core [54]; this phenomenon is called neutrino trapping. While neutrinos produced by electron capture

remain in the inner core for the order of 10 msec, the lepton fraction Y_L, the lepton number per nucleon [$Y_L \equiv (n_{\rm e} + n_\nu)/(n_{\rm n} + n_{\rm p})$ where $n_{\rm e}$, n_ν, $n_{\rm n}$ and $n_{\rm p}$ are the number densities of electrons, neutrinos, neutrons and protons], stays in a range of about 0.3 - 0.4. Trapped neutrinos build up a degenerate sea, which suppresses electron capture. Because the time scale of weak interaction processes is much shorter than $\tau_{\rm dyn} \sim \tau_{\rm diff}$, matter in the inner core is in β equilibrium with trapped neutrinos. At densities $\rho \lesssim \rho_0$, matter consists of nuclei, electrons (to maintain charge neutrality) and neutrinos, and we shall refer to this simply as supernova matter (SNM) [8, 29]. We show particle number density profiles in supernova matter in Fig. 1-(b). Since degenerate electrons are relativistic, screening effects are negligible and the electrons are uniformly distributed [37, 49, 62]. There also exist the uniform neutrino gas and neutron-rich nuclei: clusters of protons and neutrons. In a certain density region below the normal nuclear density, supernova matter could consist of nuclei with exotic shapes such as rod-like and slab-like nuclei rather than spherical ones, which are referred to as nuclear "pasta" (a further explanation will be given in Section 1.3.). The pasta nuclei affect neutrino opacity of the supernova matter (see Section 1.4.).

1.2. Neutron Stars

Let us see further evolution of the bounced core. After bounce, the core settles into hydrostatic equilibrium on its dynamical time scale and a protoneutron star is formed unless the core is not so heavy that it collapses to a black hole. The initial radius and temperature of the protoneutron star are $\sim$ 100 km and $\sim$ 10 MeV, respectively. Just after the bounce of the core, the proton fraction $x \equiv n_{\rm p}/(n_{\rm n} + n_{\rm p})$, and the lepton fraction of matter in the core are relatively high (both are around 0.3). As neutrinos escape from the protoneutron star, it cools down and electron capture, which is blocked by the degenerate neutrinos, proceeds (see, e.g., Ref. [73] for a recent review of cooling of neutron stars). Consequently matter gets neutron rich; the proton fraction $x \lesssim 0.1$ at around the normal nuclear density ρ_0. At the same time, the radius of the object shrinks to $\sim$ 10 km; a neutron star is formed.

Neutron stars are dense and compact objects supported by neutron degeneracy pressure and nuclear forces. The mass and the radius of a typical neutron star are $\simeq 1.4 M_\odot$ and $\simeq$ 10 km, respectively. The properties of dense matter and its equation of state are relatively well understood in the density region below $\sim \rho_0$. Thus the theoretical picture of neutron star structure is reasonably established in the lower density region (see, e.g., Ref. [32, 49] for reviews).

In Fig. 2 we show a schematic cross section of a typical cold neutron star below 10^9 K. The outermost part, the envelope, is a layer about several meters thick which consists of liquid ^{56}Fe (if there is accretion from its companion star, the envelope is covered by a layer of hydrogen and helium atoms). With increasing density (i.e., proceeding to the deeper region), weak interactions render nuclei neutron-rich via electron captures triggered by a large electron chemical potential. Matter becomes solid at a density $\rho \gtrsim 10^6 {\rm g\,cm^{-3}}$, which consists of nuclei forming a bcc Coulomb lattice neutralized by a roughly uniform electrons. Then, at a density of about $\sim 4 \times 10^{11} {\rm g\,cm^{-3}}$, nuclei become so neutron rich that the last occupied neutron levels are no longer bound; neutrons begin to drip out of these nuclei. These "dripped" neutrons form a superfluid amid the neutron-rich nuclei. The crystalline region of the star is referred to as crust, which is divided into inner and outer crust;

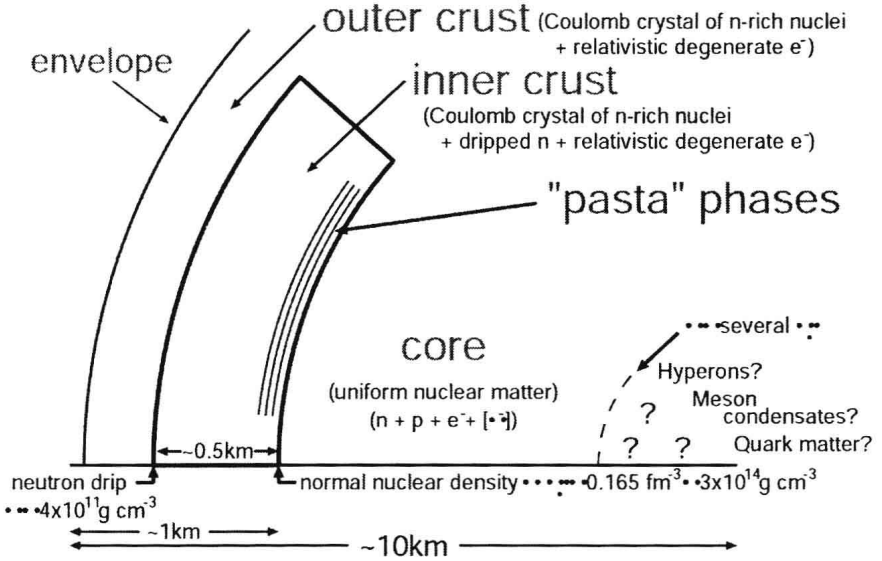

Figure 2. (Color) Schematic picture of the cross section of a neutron star.

in the outer crust there are no neutrons outside nuclei, while in the inner crust there are. The inner crust extends from the neutron drip point to the boundary with the core at a density $\rho \lesssim \rho_0 \simeq 3 \times 10^{14} \mathrm{g\,cm^{-3}}$, where nuclei disappear and the system becomes uniform nuclear matter. Matter in these regions is called neutron star matter (NSM) [5, 7, 39]. A schematic picture of neutron star matter at subnuclear densities is shown in Fig. 1-(a). There exist dripped neutrons outside the neutron-rich nuclei. Degenerate electrons are uniformly distributed for the same reason as in the case of supernova matter. Another difference between supernova matter and neutron star matter is the lack of trapped degenerate neutrinos. This makes neutron star matter more neutron-rich than supernova matter in β equilibrium. In the deepest region of the inner crust corresponding to subnuclear densities (i.e., $\rho \lesssim \rho_0$), pasta nuclei could appear (see Section 1.3. for a further explanation). Although crusts of neutron stars are relatively thin ($\sim$ 1 km), they influence many observed phenomena [32, 49]. Effects of the pasta phases on these phenomena will be discussed in Section 1.4..

The physics of the density region above several times normal nuclear density is quite uncertain, and a variety of hadronic phases have been proposed, such as hyperonic matter, pion or kaon condensates, quark-hadron mixed phase and uniform quark matter, etc. (see, e.g., Ref. [21] and references therein for details). These are beyond the scope of the present article.

1.3. What is Nuclear "Pasta"?

In ordinary matter, atomic nuclei are roughly spherical. This may be understood in the liquid drop picture of the nucleus as being a result of the forces due to the surface tension of nuclear matter, which favors a spherical nucleus, being greater than those due to the electrical repulsion between protons, which tends to make the nucleus deform. When the density of matter approaches that of atomic nuclei, i.e., the normal nuclear density ρ_0,

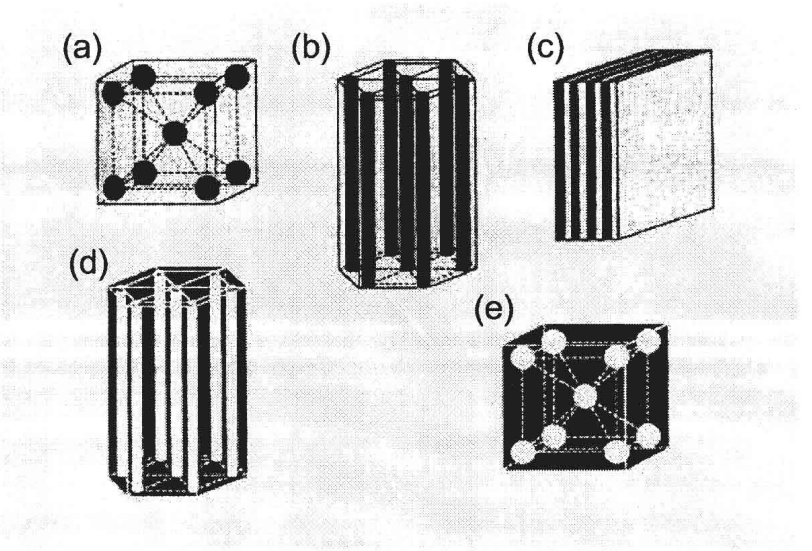

Figure 3. Nuclear "pasta." The darker regions show the liquid phase, in which protons and neutrons coexist (i.e., the nuclear matter region); the lighter ones the gas phase, which is almost free of protons. Sequence (a)-(e) shows that of nuclear shape changes with increasing density. This figure is taken from Ref. [44].

nuclei are closely packed and the effect of the electrostatic energy becomes comparable to that of the surface energy. Consequently, at subnuclear densities around $\rho \lesssim \rho_0/2$, the energetically favorable configuration is expected to have remarkable structures as shown in Fig. 3; the nuclear matter region (i.e., the liquid phase of mixture of protons and neutrons) is divided into periodically arranged parts of roughly spherical (a), rod-like (b) or slab-like (c) shape, embedded in the gas phase and in a roughly uniform electron gas. Besides, there can be phases in which nuclei are turned inside out, with cylindrical (d) or spherical (e) bubbles of the gas phase in the liquid phase. As mentioned in the previous section, these transformations are expected to occur in the deepest region of neutron star inner crusts and in the inner cores of collapsing stars just before the star rebounds. Since slabs and rods look like "lasagna" and "spaghetti", the phases with non-spherical nuclei are often referred to as "pasta" phases and such non-spherical nuclei as nuclear "pasta." Likewise, spherical nuclei and spherical bubbles are called "meatballs" and "Swiss cheese", respectively.

More than twenty years ago, Ravenhall *et al.* [52] and Hashimoto *et al.* [20] independently pointed out that nuclei with such exotic shapes [2] can be the most energetically stable due to the subtle competition between the nuclear surface and Coulomb energies as mentioned above. Let us here show this statement by a simple calculation using an incompressible liquid-drop model (see also Ref. [45]).

We consider five phases depicted in Fig. 3, which consist of spherical nuclei, cylindrical nuclei, planar nuclei, cylindrical bubbles and spherical bubbles, respectively. Each phase is taken to be composed of a single species of nucleus or bubble at a given nucleon density ρ averaged over the space. The total electrostatic energy including the lattice energy, which

[2] The "Swiss cheese" phase was considered earlier in Ref. [5] than the other pasta phases.